Experimental Test of Closed-Form EGN Model over C+L Bands

Yanchao Jiang[(1)], Antonino Nespola[(2)], Alberto Tanzi[(3)], Stefano Piciaccia[(3)], Mahdi Ranjbar Zefreh[(3)], Fabrizio Forghieri[(3)], Pierluigi Poggiolini[(1)]

[(1)] DET, Politecnico di Torino, C.so Duca Abruzzi 24, 10129, Torino, Italy, yanchao.jiang@polito.it
[(2)] LINKS Foundation, Via Pier Carlo Boggio 61, 10138, Torino, Italy
[(3)] CISCO Photonics Italy srl, via Santa Maria Molgora 48/C, 20871, Vimercate (MB), Italy

Abstract *We present a series of experiments testing a closed-form ultra-wide-band EGN model, carried out over a 5-span full C+L transmission line. Transmission ranged from quasi-linear to deeply non-linear with significant ISRS. We found quite good correspondence between predicted and measured performance.*

Introduction

In optical networking, it has become crucial to incorporate the physical-layer behavior into the network design, management, control and optimization processes. To this end, researchers have developed physical-layer models (PLMs), which have achieved significant success in accurately predicting physical-layer behavior. These PLMs have been extensively utilized in the industry for some time, with the GN and EGN models being among the most widely adopted.

Recently, though, the requirements on PLMs have been stepped up significantly. They now ask for faster computation speeds for iterative optimization and real-time management, as well as the ability to account for frequency-dependent parameters due to the extension of the usable fiber bandwidth to ultra-wide-band (UWB) [1], [2].

To address these challenges, approximate closed-form models (CFMs) have been developed, capable of real-time computation, with support of UWB by including the frequency-dependence of all key parameters and of Inter-channel Raman scattering (ISRS). Two groups, one at UCL and one at PoliTo (in collaboration with CISCO) have independently obtained UWB-enabled CFMs that are based on the GN and EGN models, with similar foundations and capabilities but with differences in features and final analytical form. For UCL-CFM see [3] (and [4]-[8]), for CISCO-PoliTo-CFM [9] (and [10]-[14])

In view of the possible use of the CISCO-PoliTo-CFM in deployed networks, we have carried out an extensive validation campaign vs. several experiments, that were carried out on a 5-span fully populated C+L system. A wide variety of propagation conditions were tested, ranging from quasi-linear to deeply non-linear. In all testing conditions the CISCO-PoliTo-CFM (henceforth just "CFM") showed quite good agreement with the experiments. In this paper we report on this experimental validation effort.

The experimental setup

The schematic is shown in Fig.1. The setup consisted of 61 channels in C-band, from 191.8 to 195.9 GHz, and 67 channels in L-band, from 186.2 to 190.8 GHz. The C+L WDM comb was generated by shaping ASE noise through programmable optical filters, emulating 52GBaud channels spaced 68.75 GHz, roll-off 0.1. For performance measurement, each emulated channel was replaced in turn by an actual PM-16QAM channel, generated by a C-band or a L-band transmitter card.

The line consisted of 5 spans of SMF each with about 86 km length. The C-band and L-band combs were separately amplified at launch and after each span. The line was instrumented so that both the full signal spectrum and the spectrally resolved OSNR could be measured at each one of the red and green probing points shown in Fig.1, numbered from "0" to "5", where 10/90 splitters were placed. This way, the frequency-dependent gain and noise figure of each EDFA could be accurately measured, while the system was operating.

The receivers were separate C and L-band units and provided hard-decision BER as well as the constellation SNR after DSP. The launched WDM spectrum into the first span could be arbitrarily shaped by means of the programmable optical filters. Each amplifier could be controlled as to its gain and tilt. This way, quite different propagation conditions could be imposed.

Setup characterization

The fibers of the setup were SMF G652D. Each span consisted of more than one spool, but the first spool in each span was at least 40km long, ensuring that non-linear effects would occur over an uninterrupted 40km fiber stretch. The five spans were individually characterized as for their attenuation and dispersion profiles vs. frequency (Fig.2). Note that the loss displayed in Fig.2 is

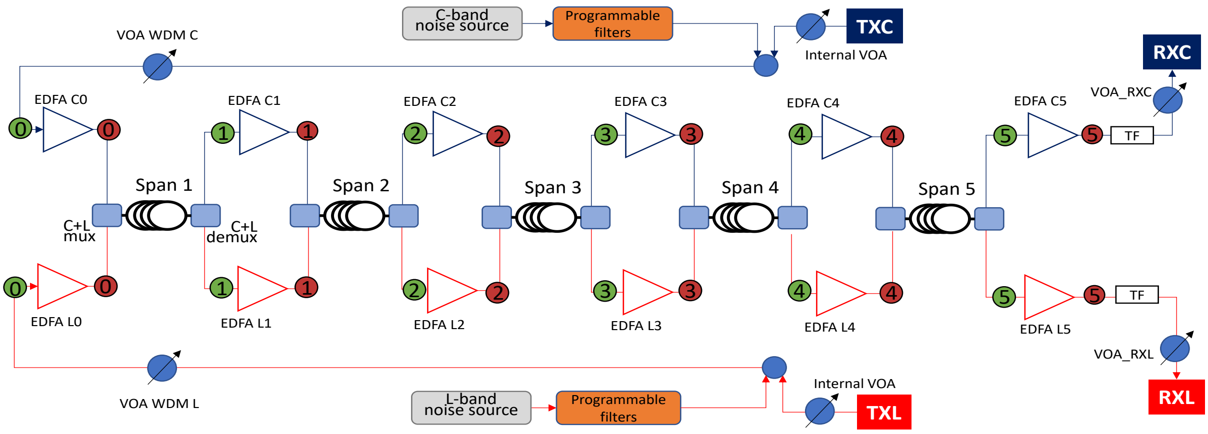

Fig. 1: General schematic of the C+L line experiment. VOA: variable optical attenuator. TF: tunable filter.

pure fiber loss (lumped loss was measured by OTDR and removed from this plot). The fiber non-linearity coefficient γ was characterized by means of a dedicated experiment based on XPM and found to essentially agree with the literature reported values of 1.25 1/(W km) at 192 THz.

As for the frequency variability of γ, the behavior described by [9], Eq.(4), was assumed. Note that the equation provides different values depending on NLI being SPM or XPM. A plot of

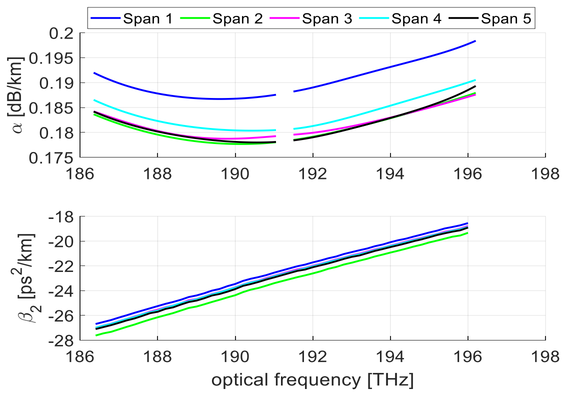

Fig. 2: (a) fiber attenuation (with lumped losses removed) and (b) dispersion, both vs. optical frequency

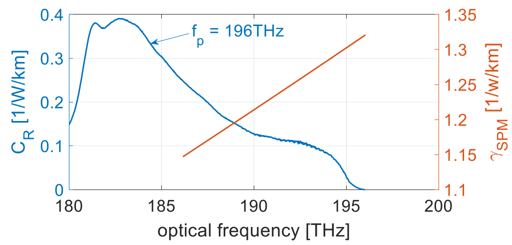

Fig. 3: Blue: Raman gain spectrum for 196 THz pump frequency. Orange: SPM non-linearity coefficient γ_{SPM}

γ_{SPM} vs. frequency is shown in Fig.3 as an example. Regarding ISRS, the Raman gain spectrum was measured at a pump frequency of 206.5 THz and then translated to different pump frequencies according to Eqs. (37)-(39) in [15]. An instance of the Raman gain spectrum due to a “pump” translated to 196 THz is shown in Fig.3.

Experimental Results

The goal of this study was to validate the CFM by comparing the GSNR predicted using the CFM ($\mathrm{GSNR_{CFM}}$) with the actual GSNR measured on all 128 channels ($\mathrm{GSNR_{meas}}$), in several different propagation regimes.

$\mathrm{GSNR_{meas}}$ was found as follows. The Rx provided $\mathrm{SNR_{meas}}$, i.e., the SNR on the constellation after DSP. $\mathrm{SNR_{meas}}$ does not coincide with $\mathrm{GSNR_{meas}}$ because of the Tx-Rx pair internal noise. They are related as follows:

$$\mathrm{GSNR_{meas}} = \mathrm{SNR_{meas}} \cdot (1 - \mathrm{SNR_{meas}}/\mathrm{SNR_{bb}})^{-1}$$

where $\mathrm{SNR_{bb}}$ is the measured constellation SNR in back-to-back (no ASE). We found $\mathrm{SNR_{bb}}$=19.9 dB for both the C and L band Tx-Rx pair.

$\mathrm{GSNR_{CFM}}$ was calculated using the CFM, based on the detailed characterization of the overall link and based on the measured signal launch power spectrum into each span. Regarding ASE noise in $\mathrm{GSNR_{CFM}}$, it was not calculated but physically measured at each channel frequency, at the input of the Rx. The reason why we chose to use measured ASE values is that our goal was CFM validation and such validation would potentially be degraded if there were errors in ASE power within $\mathrm{GSNR_{CFM}}$.

To provide another independent comparison, we also calculated $\mathrm{GSNR_{EGN}}$ with NLI predicted using the full-fledged, numerically integrated EGN model, including ISRS and all frequency-dependent quantities too [14].

Fig.4 shows the results of the comparison among $\mathrm{GSNR_{meas}}$, $\mathrm{GSNR_{CFM}}$ and $\mathrm{GSNR_{EGN}}$ in four different regimes. In Fig.4(a) the results for quasi-linear transmission are shown. Here ASE prevails over NLI and therefore OSNR (black dots), which includes only ASE noise, is only 1dB above $\mathrm{GSNR_{meas}}$ (blue dots). The correspondence between CFM and EGN predictions with the measurements is excellent, but in this regime NLI power is low (only ¼ of ASE power) and possible CFM inaccuracy would be largely masked.

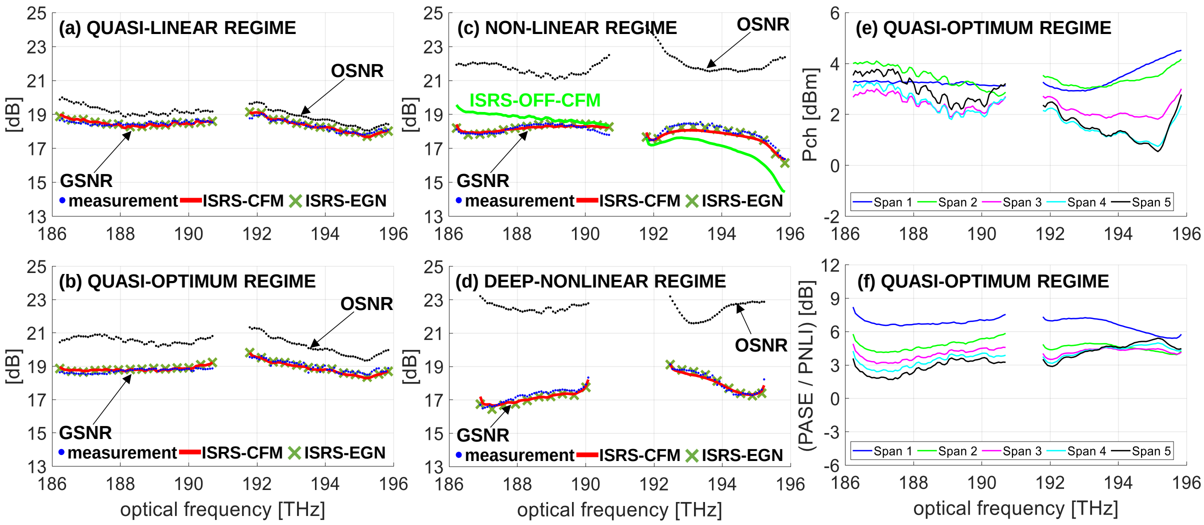

Fig. 4: (a),(b),(c),(d): four different system scenarios with increasing amount of non-linearity. Black dots: measured OSNR (ASE only). Blue dots: measured GSNR (ASE+NLI). Red lines: closed-form-model predictions of GSNR. (e), (f): launch power into each span and measured PASE/PNLI ratio at the output of each span, for the scenario (b).

We then increased the launch power into each span to achieve a more non-linear propagation. We chose as approximate target $P_{ASE}/P_{NLI} \approx 3$dB which is the ratio that maximizes GSNR [16], [17] in an ideal homogeneous link. It corresponds to an OSNR vs. GSNR gap of 1.8 dB and the results shown in Fig.4(b) are close to this value. To approach this target ratio, the launch power into each span was tailored based on a digital twin of the link obtained through its detailed characterization and the CFM. The measured launched power spectrum into each span is shown in Fig. 4(e), clearly affected by EDFAs ripples which was not possible to eliminate. We also measured the P_{ASE}/P_{NLI} ratio after each span Fig.4(f). Note that it starts out higher than 3dB and then it tends to converge to 3dB towards the end of the link. The reason for this trend is that a non-negligible amount of ASE was already present in the signal before entering the link (OSNR$\approx$26.4dB in L band and $\approx$27.8dB in C band at the red dot with "0" in Fig.1), skewing the P_{ASE}/P_{NLI} ratios upward in the first spans.

In this scenario too, the CFM accuracy appears very good, with $\mathrm{GSNR}_{\mathrm{CFM}}$ within ±0.3 dB of the $\mathrm{GSNR}_{\mathrm{meas}}$. Also, $\mathrm{GSNR}_{\mathrm{CFM}}$ and $\mathrm{GSNR}_{\mathrm{EGN}}$ are almost perfectly aligned showing that, despite the many approximations involved in the CFM derivation, accuracy is largely preserved.

We then turned up the launch power to achieve highly non-linear regimes. The purpose was to stress-test the CFM accuracy. In Fig.4(c) we achieved on average OSNR/GSNR$\approx$4dB. We then tried to push the link even further into non-linearity, but we were limited by the power available at the EDFAs. To increase the launch power per channel, we reduced the number of channels to 47 and 41 in the L and C bands, respectively. Thanks to this, we managed to further widen the gap between OSNR and GSNR, especially in the low L-band and high C-band, where we reached OSNR/GSNR$\approx$6dB, see Fig.4(d). The CFM predictions remained quite accurate, also in these challenging regimes where GSNR is prevalently set by NLI and hence by the CFM, to within ±0.5dB of $\mathrm{GSNR}_{\mathrm{meas}}$. $\mathrm{GSNR}_{\mathrm{CFM}}$ and $\mathrm{GSNR}_{\mathrm{EGN}}$ kept being almost coincident. To appreciate the importance of accurate ISRS modelling in C+L systems, in Fig.4(c) we show $\mathrm{GSNR}_{\mathrm{CFM}}$ with ISRS off (green). The gap between predicted and measured GSNR shoots up to almost 2 dB in the low L-band and high C-band, showing how critical ISRS is.

We also performed several other tests, such as targeting max GMI or flattest GSNR, which we cannot report here due to lack of space. $\mathrm{GSNR}_{\mathrm{CFM}}$ was always within ±0.5 dB of $\mathrm{GSNR}_{\mathrm{meas}}$.

Discussion and Conclusion

We tested the accuracy of a closed-form non-linearity model (CFM) developed by CISCO and PoliTo, by means of a dedicated 5-span C+L in-line experiment. The model accounts for ISRS as well as for the frequency-dependence of all relevant fiber parameters. We found that the CFM accuracy is quite good, over several different propagation regimes, from weakly non-linear to highly non-linear. The challenge to obtain an accurate prediction of the GSNR at the end of the system was found to be due more to uncertainty in the characterization of amplifiers, fibers and other components, rather than CFM accuracy.

In conclusion, from the viewpoint of non-linearity modelling, the CISCO-PoliTo-CFM appeared to be quite reliable, across the whole C+L band, and potentially accurate enough for possible practical use.

References

[1] J. Renaudier *et al.*, "Devices and Fibers for Ultrawideband Optical Communications," *Proc. IEEE*, vol. 110, no. 11, pp. 1742–1759, 2022, doi: 10.1109/JPROC.2022.3203215.

[2] T. Hoshida *et al.*, "Ultrawideband Systems and Networks: Beyond C + L-Band," *Proc. IEEE*, vol. 110, no. 11, pp. 1725–1741, 2022, doi: 10.1109/JPROC.2022.3202103.

[3] H. Buglia *et al.*, "A Closed-Form Expression for the Gaussian Noise Model in the Presence of Inter-Channel Stimulated Raman Scattering Extended for Arbitrary Loss and Fibre Length," *J. Light. Technol.*, pp. 1–10, 2023, doi: 10.1109/JLT.2023.3256185.

[4] D. Semrau, G. Saavedra, D. Lavery, R. I. Killey, and P. Bayvel, "A Closed-Form Expression to Evaluate Nonlinear Interference in Raman-Amplified Links," *J. Light. Technol.*, vol. 35, no. 19, pp. 4316–4328, Oct. 2017, doi: 10.1109/JLT.2017.2741439.

[5] D. Semrau, R. I. Killey, and P. Bayvel, "A Closed-Form Approximation of the Gaussian Noise Model in the Presence of Inter-Channel Stimulated Raman Scattering." Aug. 23, 2018. [Online]. Available: https://arxiv.org/abs/1808.07940

[6] D. Semrau, R. I. Killey, and P. Bayvel, "A Closed-Form Approximation of the Gaussian Noise Model in the Presence of Inter-Channel Stimulated Raman Scattering," *J. Light. Technol.*, vol. 37, no. 9, pp. 1924–1936, May 2019, doi: 10.1109/JLT.2019.2895237.

[7] D. Semrau, E. Sillekens, R. I. Killey, and P. Bayvel, "A Modulation Format Correction Formula for the Gaussian Noise Model in the Presence of Inter-Channel Stimulated Raman Scattering," *J. Light. Technol.*, vol. 37, no. 19, pp. 5122–5131, Oct. 2019, doi: 10.1109/JLT.2019.2929461.

[8] D. Semrau, "Modeling of Fiber Nonlinearity in Wideband Transmission," in *OFC 2022*, San Diego (CA), Mar. 2022, p. paper W3C.6.

[9] P. Poggiolini and M. Ranjbar-Zefreh, "Closed Form Expressions of the Nonlinear Interference for UWB Systems," in *2022 European Conference on Optical Communication (ECOC)*, 2022, p. Tu1D.1.

[10] P. Poggiolini, G. Bosco, A. Carena, V. Curri, Y. Jiang, and F. Forghieri, "The GN model of fiber non-linear propagation and its applications," *J Light. Technol*, vol. 32, no. 4, pp. 694–721, Feb. 2014.

[11] P. Poggiolini, "A Generalized GN-Model Closed-Form Formula." Sep. 24, 2018. [Online]. Available: https://arxiv.org/abs/1810.06545v2

[12] M. Ranjbar Zefreh, F. Forghieri, S. Piciaccia, and P. Poggiolini, "Accurate Closed-Form Real-Time EGN Model Formula Leveraging Machine-Learning Over 8500 Thoroughly Randomized Full C-Band Systems," *J. Light. Technol.*, vol. 38, no. 18, pp. 4987–4999, Sep. 2020, doi: 10.1109/JLT.2020.2997395.

[13] M. Ranjbar Zefreh and P. Poggiolini, "A Real-Time Closed-Form Model for Nonlinearity Modeling in Ultra-Wide-Band Optical Fiber Links Accounting for Inter-channel Stimulated Raman Scattering and Co-Propagating Raman Amplification," *ArXiv Prepr. ArXiv200603088*, Jun. 2020, doi: 10.48550/arXiv.2006.03088.

[14] M. Ranjbar Zefreh and P. Poggiolini, "Characterization of the Link Function in GN and EGN Methods for Nonlinearity Assessment of Ultrawideband Coherent Fiber Optic Communication Systems with Raman Effect," *ArXiv Prepr. ArXiv200912687*, Oct. 2020, doi: https://doi.org/10.48550/arXiv.2009.12687.

[15] K. Rottwitt, J. Bromage, A. J. Stentz, L. Leng, M. E. Lines, and H. Smith, "Scaling of the Raman gain coefficient: applications to germanosilicate fibers," *J. Light. Technol.*, vol. 21, no. 7, pp. 1652–1662, Jul. 2003, doi: 10.1109/JLT.2003.814386.

[16] G. Bosco, A. Carena, R. Cigliutti, V. Curri, P. Poggiolini, and F. Forghieri, "Performance prediction for WDM PM-QPSK transmission over uncompensated links," in *Proc. Opt. Fiber Commun. Conf. (OFC)*, 2011, pp. 1–3.

[17] E. Grellier and A. Bononi, "Quality parameter for coherent transmissions with Gaussian-distributed nonlinear noise," *Opt. Express*, vol. 19, no. 13, pp. 12781–12788, 2011.